PHYSICAL REVIEW A VOLUME 24, NUMBER 4 OCTOBER 1981

$2s$-$2p$ transitions in heliumlike ions

R. DeSerio,* H. G. Berry, R. L. Brooks, and J. Hardis†
Argonne National Laboratory, Argonne, Illinois 60439

A. E. Livingston and S. J. Hinterlong
University of Notre Dame, Notre Dame, Indiana 46556
(Received 22 May 1981)

Precision wavelength measurements are presented for the $1s\,2s\ ^3S_1$-$1s\,2p\ ^3P_{0,2}$ transitions of silicon, sulfur, and chlorine. Calculations have been made for these transitions using a double expansion in Z^{-1} and α^2Z^2. These calculations include the nonrelativistic energy, one-electron Dirac energy, plus relativistic corrections and the Breit interaction calculated in first-order perturbation theory in both high-Z and low-Z approximations. After considering the one-electron Lamb-shift corrections to high order, comparison with our measurements and with other experiments for $Z=4-26$ reveals a discrepancy which is approximately $0.015Z^3$ cm^{-1}. We show that this can arise from two-electron quantum electrodynamic corrections to the one-electron Lamb shift and we derive an *ab initio* estimate of this correction in good agreement with the observations.

I. INTRODUCTION

In one-electron atoms, the Dirac equation plus existing quantum electrodynamic (QED) calculations accurately predict the observed atomic energy levels. However, there is no closed-form analog to the Dirac Hamiltonian to describe two-electron (or more) atoms. In addition, in all currently successful atomic theories, QED corrections are only added perturbatively, although bound-state propagators have been used for accurate calculations[1-4] of some of the QED-type corrections in one-electron systems. For ions of low nuclear charge Z, relativistic effects are generally combined with the Breit interaction in a Breit-Pauli Hamiltonian which is useful in obtaining their contributions to first order using perturbation theory.[5] When Z is very large the electron-nucleus interactions dominate over the electron-electron interactions. In these systems, we can first consider the electrons to be noninteracting and bound to the nucleus according to the relativistic Dirac equation. The electron-electron interactions and QED corrections can then be treated perturbatively.[6]

In this work, we have combined the best existing calculations following the perturbation theories appropriate to the low-Z region with a new calculation of the perturbation theory appropriate to the high-Z region. The combination is applied to the $\Delta n=0$, $n=2$ state transitions of the two-electron heliumlike isoelectronic sequence, and provides results which are applicable to the range of ions for $Z=2-50$.

We also present some new precision measurements of the transitions $1s\,2s\ ^3S_1$-$1s\,2p\ ^3P_{0,2}$, in the heliumlike ions of silicon, sulfur, and chlorine. We have compared all measurements for these transitions in the heliumlike ions for $Z=4-26$, with our theoretical results. Agreement between theory and experiment is obtained when we include a first-order correction to the one-electron QED contributions. We discuss our estimate of this correction in the two-electron system and the improvements which might be possible in atomic structure calculations for more general many-electron systems.

II. EXPERIMENT

A. General

The experiment is a standard beam-foil excitation measurement using fast beams ($v/c\approx0.08$) of silicon and sulfur from the Argonne FN tandem accelerator impinging on a thin foil in a target chamber as shown schematically in Fig. 1. Most of the experimental details have been described previously.[7,8] The observed transitions were measured with a 1-m normal incidence monochromator, positioned to view the radiation emitted near 90° to

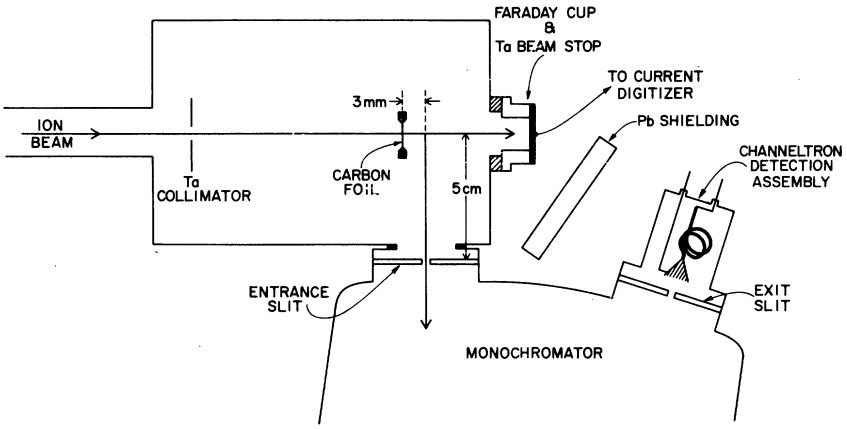

FIG. 1. Experimental geometry.

the beam direction. We determine the fine-structure transition wavelengths by measuring their wavelength separations either to previously measured transitions, or to transitions connecting high-lying Rydberg levels. These latter wavelengths can be calculated accurately. The problems associated with this technique are monochromator calibration,[9] proper accounting of Doppler shifts, and careful evaluation of mean wavelengths of the fine-structure components of the calibration lines. We consider these three problems below. The 1200 lines/mm grating used for the sulfur measurements was blazed at 150 nm and overcoated with osmium. For the silicon measurements, an osmium-overcoated grating blazed at 250 nm was used. These overcoatings increased the reflectivity of the gratings below 100 nm. The blaze wavelengths enhanced the reflectivity for the orders of diffraction in which the transitions were measured.

We reduced the large Doppler broadening expected in perpendicular viewing of fast-beam light sources with a monochromator focused for a stationary source by employing the method of fast-beam refocusing.[10] We made adjustment to a pivoting cam which controls the distance from the grating to the exit slit, thus refocusing the monochromator at all wavelengths for a particular beam velocity. This procedure was performed once at the beginning of an experiment, for a beam velocity representing an intermediate value to those actually used. (Typically $v/c=0.07$ was chosen.) This was done for convenience and to ensure precise calibration. Repeating the procedure for each change in beam velocity (typically four or five different energies were used for each experiment) would have used up valuable beam time (the monochromator has to be opened and then allowed sufficient time to reach an operating vacuum of about 1×10^{-6} torr). More importantly, wavelength calibration of the monochromator is then done with the monochromator in the same refocused configuration as used in the experiment.

In order that the best reproducibility be attained when making multiple scans with the monochromator over the same wavelength region, a computer-controlled stepping motor was interfaced to the monochromator. At the end of each scan the computer automatically reset the wavelength drive before beginning the next scan. Typical reproducibility, as measured by the position of strong transitions on multiple runs, was better than 0.002 nm.

B. Monochromator calibration

Our calibration procedure[9] allows us to accurately correct for the effects of nonlinearities in the grating drive mechanism, which cause small periodic variations in the dispersion, correlated with the rotation of the grating drive screw of the monochromator. In addition, it provides an accurate check on the value of the linear dispersion coefficient, nominally 2.5 nm per revolution of the drive screw.

For calibration of the monochromator dispersion, we measured line spectra between 85 and 200 nm from a windowless argon discharge lamp with the monochromator in both a refocused[10] and a nonrefocused configuration. The measurements resulted in a wavelength deviation from the standard constant dispersion of

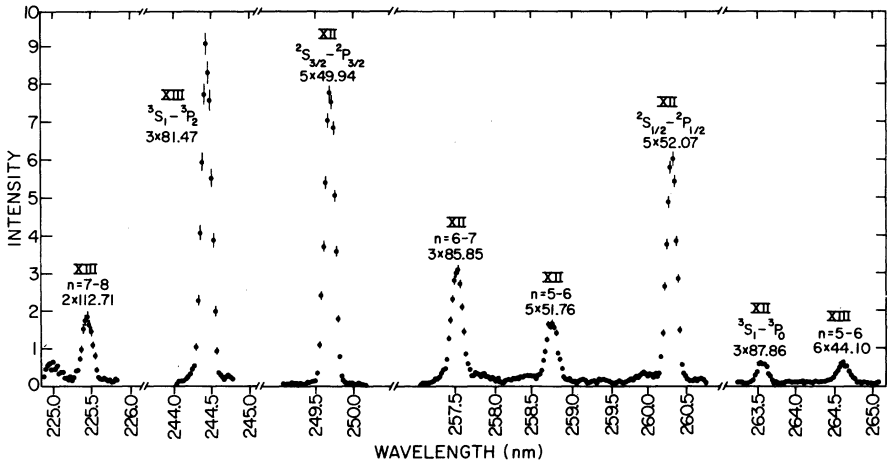

FIG. 2. Sample spectra used in the Si XIII $1s2s\ ^3S_1$-$1s2p\ ^3P_{0,2}$ wavelength determinations.

$$\Delta\lambda = \lambda_0 + k\lambda_M + (A + B\lambda_M)\sin[(\lambda_M - \lambda_\phi)2\pi/2.5] , \quad (1)$$

where λ_0 is the *offset error* of the zero-wavelength reading, $k\lambda_M$ is a *linear error* in the measured wavelength λ_M due mainly to a misadjustment of the grating lever cam, and the constants A, B, and λ_ϕ describe a *periodic error* due principally to different modes of wobble in the screw rotation of the grating drive.

The linear error was small ($k \lesssim 3\times 10^{-5}$), while the peak-to-peak periodic error was typically 0.010 nm. Reproducibility of wavelengths was typically better than 0.002 nm.

C. Calibration lines

The beam-foil light source has long been known[11] to strongly populate Rydberg states of high (n,l). Because of the small interaction with the core electrons for the nonpenetrating orbits, the energy of these Rydberg states is nearly hydrogenlike and can be easily calculated. Thus, these transitions are especially suited as calibration lines in beam-foil spectra, as suggested previously.[12,13]

For the energies used in these experiments such Rydberg transitions are observed for ion species containing 2–5 electrons, as can be seen in Fig. 2. The term energies contributing to these transitions are generally described[14] as the sum of a hydrogenic term T_H obtained from the Sommerfeld formula plus a core polarization term Δp corresponding to multipole interactions of the Rydberg electron with the core. For two-electron ions the $1s$ core polarizability can be calculated nonrelativistically from the Schrödinger wave functions,[15]

$$A = (9/2)[(Z-1)/Z]^4 , \quad (2)$$

$$k = (10/3)[(Z-1)/Z]^2 , \quad (3)$$

where A and k are the dipole and quadrupole factors as defined in Ref. 14.

For a three-electron ion, the $1s^2$ core polarizability is approximated by an empirical fit to measured transitions in lower-Z ions,[16]

$$A = 9(Z-2)^4(Z-s)^{-4} , \quad (4)$$

$$kA^{-1/2} = 0.2113Z + 0.598 - 2.4Z^{-1} , \quad (5)$$

where s is a screening parameter given by

$$s = 0.3397 + 0.102(Z-0.4)^{-1} . \quad (6)$$

Some comparisons between theory and experiments of these formulas in high-Z three-electron systems have been made by Edlén.[16] In particular, the $4f$-$5g$ transitions in Si XII show agreement at the precision of the experiment (± 5 cm^{-1}). Because the effects of Dirac fine structure and the fine structure contributed by differing core interactions for differing l sublevels are small, the observed transitions generally have fine-structure components whose separations are well below the experimental resolutions. We have estimated the cumulative effect of this fine structure. Each wavelength within the given n,n' transition is weighted according to its hydrogenic transition probability and according to

two schemes for the population of the upper state.

Statistical $(2l+1)$ populations may be expected and have been observed in previous beam-foil measurements.[17] However, some observations[13] have shown population distributions which increase more strongly with l. Thus the weighted mean wavelengths are calculated with both a $2l+1$ and an l^2 weighting for the upper level.

Because the yrast transition ($n,l=n-1$ to $n'=n-1,l'=l-1$) gives the major contribution to the total line intensity and because the splittings of other members which contribute appreciably are small, the calculated mean wavelengths are not strongly dependent on the weighting of the upper level. We have decided to use the statistical weighting and take the difference from the l^2 weighting to be an estimate of the associated error. Because of the difference in the lifetimes of the individual fine-structure states, these populations will vary as a function of the distance downstream from the foil, i.e., the time from excitation. For an ion velocity of $0.07c$ these changes in population produce shifts in the mean transition wavelength on the order of $+0.001$ nm/cm. In these measurements, we collect the light emitted over the first 3 mm of the decay, which typically implies a correction of about $+0.0003$ nm. We estimate an error from this effect of 0.0005 nm, which is much smaller than the wavelength uncertainty due to the initial population distribution. An associated effect is due to the nonuniform intensity of the light source over the observed beam length, due to the decay in flight of the moving ions. This can produce a lifetime-dependent Doppler shift of the observed wavelength. For the transitions observed, the shift is less than 0.0005 nm.

The estimated contributions to the uncertainties in the absolute wavelengths of the observed hydrogenic calibration lines are summarized below:

Population: 0.001–0.002 nm,
Mean life: 0.0007 nm,
Profile asymmetry: 0.001 nm,
Polarizability: 0.001–0.002 nm,
Total: 0.002–0.003 nm.

The polarizability uncertainty is one-half the total wavelength change due to the polarizability and is certainly an overestimate.

In addition to these hydrogenic transitions, it was found worthwhile to use as calibration lines other previously measured transitions. The resonance lines ($1s^2 2s\ ^2S_{1/2}$-$1s^2 2p\ ^2P_{1/2,3/2}$) in three-electron silicon and sulfur were observed in our spectra, and they have been measured previously in both laboratory spectra[18,19] and in solar flares.[20,21] A weighted average from these four references for the sulfur resonance lines is used; $\lambda(^2S_{1/2}-{}^2P_{1/2})=44.572\pm0.003$ nm, $\lambda(^2S_{1/2}$-$^2P_{3/2})=41.766\pm0.002$ nm. For silicon the weighted mean wavelengths for these transitions, as reported in Refs. 20–22, are 52.069 ± 0.003 and 49.940 ± 0.003 nm, respectively. For the sulfur spectra, the wavelength of the $1s^2 2s\,2p\ ^1P^0$-$1s^2 2p^2\ ^1D$ transition is given by Fawcett[19] as 50.042 ± 0.003 nm.

TABLE I. Calibration lines used in the experiments.

Transition	Wavelength (nm)
Si XIII $n=5$-6	44.097±0.003
Si XIII $n=7$-8	112.710±0.003
Si XII $n=5$-6	51.762±0.002
Si XII $n=6$-7	85.851±0.003
Si XII ^2S-$^2P_{1/2}$	52.069±0.003
Si XII ^2S-$^2P_{3/2}$	49.940±0.003
S XIV $n=6$-7	63.070±0.002
S XIV $n=7$-8	97.179±0.003
S XIV ^2S-$^2P_{1/2}$	44.572±0.003
S XIV ^2S-$^2P_{3/2}$	41.766±0.003
S XIII ^1P-^1D	50.042±0.003
Cl XV $n=8$-9	123.477±0.003
Cl XIV $n=8$-9	70.61±0.02

Table I summarizes the wavelengths and their uncertainties for the calibration lines used in these experiments.

D. Doppler shift

Having obtained the dispersion of the monochromator, we can accurately determine the wavelength separation between any two measured transitions, which, however, will be dependent on the Doppler shifts of the lines themselves.

The Doppler formula gives the measured wavelength, λ_m:

$$\lambda_m=\lambda_0\gamma(1-\beta\cos\theta)\ , \tag{7}$$

where $\gamma=1+E/mc^2$, $\beta=(1-1/\gamma^2)^{1/2}$. E is the kinetic energy of the beam, m is the mass of the ion, θ is the angle between the beam direction and the optical axis of the monochromator, and λ_0 is the wavelength at zero velocity of the source.

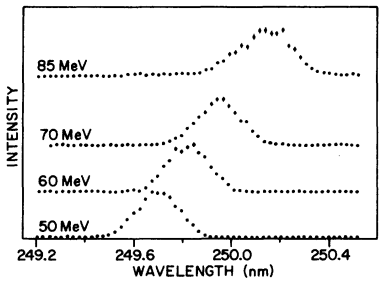

FIG. 3. Doppler shifts of the $1s^2 2s\ ^2S_{1/2}$-$1s^2 2p\ ^2P_{3/2}$ transition in Si XII as a function of beam energy.

Thus, the Doppler-free wavelength separation between two transitions $\Delta\lambda_0$ is

$$\Delta\lambda_0 = \lambda_0^{(1)} - \lambda_0^{(2)} = \Delta\lambda_m / \gamma(1-\beta\cos\theta) , \quad (8)$$

where the m subscript refers to measured wavelengths and

$$\Delta\lambda_m = \lambda_m^{(1)} - \lambda_m^{(2)} . \quad (9)$$

In this way we can then use a calibration line, for example, $\lambda_0^{(2)}$, to obtain the desired zero-velocity wavelength of, for example, $\lambda_0^{(1)}$:

$$\lambda_0^{(1)} = \lambda_0^{(2)} + \Delta\lambda_m / \gamma(1-\beta\cos\theta) . \quad (10)$$

It is therefore important to know the value of this Doppler factor $\gamma(1-\beta\cos\theta)$ as accurately as possible. Limits on its accuracy are imposed by uncertainties in the beam energy E and the angle θ. Our uncertainty in E (<300 keV) affects the Doppler factor through the energy dependence of γ and $\beta\cos\theta$, and both effects are very small. They are approximately 1×10^{-5} for γ and 2×10^{-6} for $\beta\cos\theta$.

The largest uncertainty in the Doppler factor is that associated with the observation angle θ. Assuming a nominal value for β of 0.07, an uncertainty in θ (for θ near 90°) results in an uncertainty in the Doppler factor of 1.2×10^{-3}/degree of uncertainty in θ.

We determined this angle by measuring the shifts in the measured wavelengths as the beam energy was varied. Figure 3 illustrates this effect on the $1s^2 2s\ ^2S_{1/2}$-$1s^2 2p\ ^2P_{3/2}$ Si XII transition measured in fifth order. The scans over each transition (eight different transitions were used in the analysis) were taken at four different energies. There is an approximately linear increase in wavelength with energy as predicted by Eq. (7) with θ near 90°.

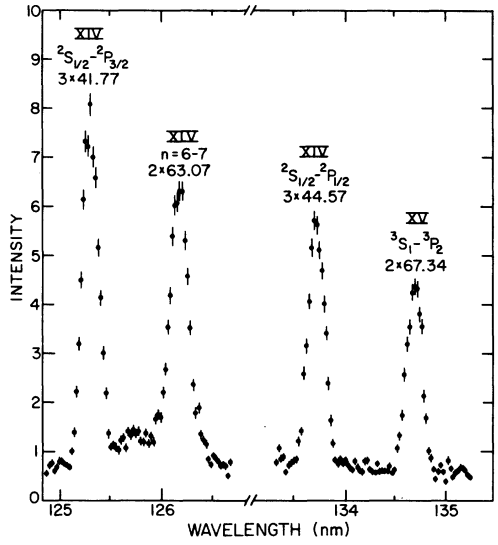

FIG. 4. Sample spectra used in the S XV $^3S_1$-$^3P_2$ wavelength determination.

Using one particular energy as a reference, the shift in the measured wavelength of the eight lines at the other three energies gives 24 independent determinations of the angle. The distribution of values has a mean of 91.0° and a one standard deviation of 0.35°.

The largest contribution to the uncertainty of a single determination of θ arises from the uncertainty in the measured wavelength shift and decreases for larger energy separation or λ_0. Taking a proper weighted average, one obtains a mean of 91.0° and a one standard deviation of 0.26°, which corresponds to uncertainties of about 0.006 nm in the measured wavelength shift. Statistically, the standard error of the mean is under ±0.05°. Because

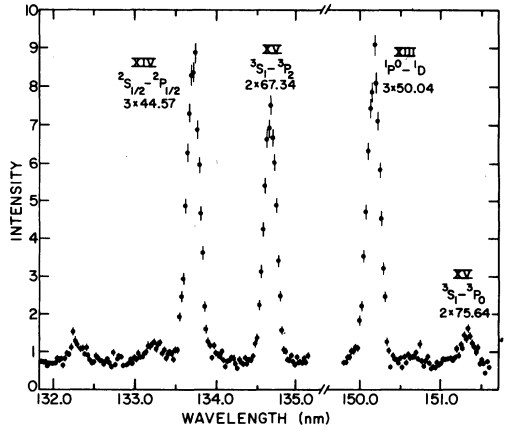

FIG. 5. Sample spectra used in the S XV $^3S_1$-$^3P_{0,2}$ wavelength determinations.

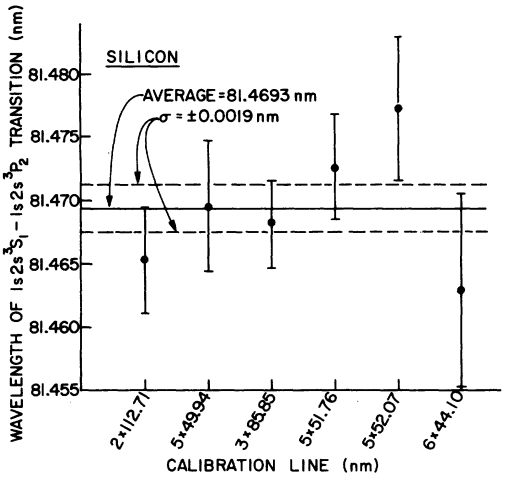

FIG. 6. Si XIII $^3S_1$-$^3P_2$ wavelengths obtained from each calibration transition.

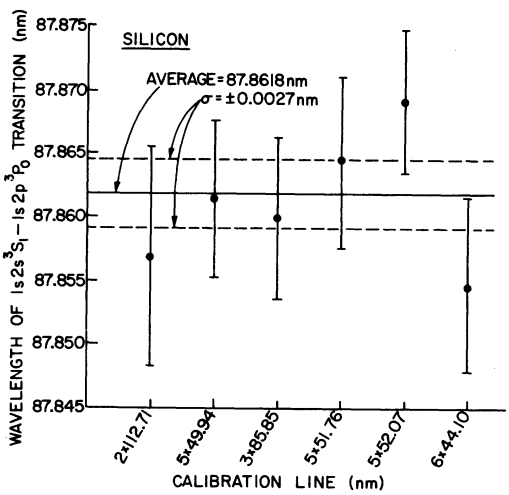

FIG. 7. Si XIII $^3S_1$-$^3P_0$ wavelengths obtained from each calibration transition.

the results do not show a Gaussian distribution we use a conservative estimate of $\pm 0.13°$.

Systematic shifts in beam energy, expected to be less than 15 keV/MeV, may have a small effect on the determination of θ ($\pm 0.06°$). The total uncertainty in θ is estimated to be 0.15°; 0.13° from statistical uncertainty, 0.06° from systematic uncertainty. This uncertainty dominates the overall uncertainty in the Doppler factor, its contribution being approximately 2.0×10^{-4}.

III. DATA ANALYSIS AND RESULTS

The data analysis was carried out using an interactive computing system at Argonne National Laboratory. All spectra (e.g., Figs. 2, 4, and 5) were fit to Gaussian profiles with position, height, width, and background parameters.

For each different run of each energy, the wavelength separations between the ^3S-^3P transitions and the calibration lines are corrected using the associated monochromator calibration curve. These corrections are typically 0—0.01 nm. The separations are then corrected by the appropriate Doppler factor for the energy of the run to obtain the Doppler-free separations. Depending on the energy at which the run was taken and the actual separation, this correction would be 0—0.05 nm.

The Doppler-free separations for all runs are then compared for scatter. Typically this scatter is on the order of 0.006 to 0.020 nm. The average is used as the true separation from the calibration line. This separation, together with the wavelength of the calibration line, determines the wavelength of the ^3S-^3P transition (in the spectral order in which it was measured). In addition to the scatter, the associated error in this final wavelength is taken as the root-mean-square sum of the following errors:

(1) An uncertainty of 0.0025 nm in the correction associated with the monochromator calibration curve.

(2) An uncertainty in the calibration lines (0.002—0.003 nm). These would be multiplied by the appropriate factor when used in higher order than the first.

(3) The error associated with the Doppler factor is taken to be 2.0×10^{-4} times the wavelength separation. Actually, this error factor varies slightly with the energy $[(1.7-2.2)\times 10^{-4}]$ and should

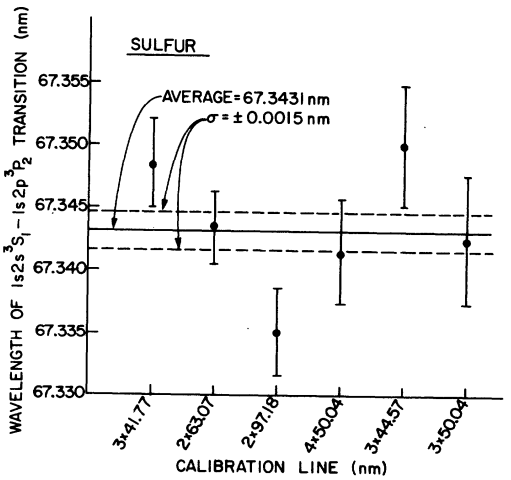

FIG. 8. S XV $^3S_1$-$^3P_2$ wavelengths obtained from each calibration transition.

be applied separately to each different energy. However, because this error is almost entirely due to the uncertainty in the observation angle, which does not change with energy, this procedure would obscure the statistical scatter in the wavelength separations, which shows a clear correlation with the intensity of the associated lines. Figures 6–8 show graphically the results of these analyses applied to the $^3S_1$-$^3P_{0,2}$ transitions in Si XIII and for the $^3S_1$-$^3P_2$ transition in S XV. For the weaker $^3S_1$-$^3P_0$ S XV transition only four spectra were used and resulted in the two determinations 75.639±0.006 nm (when compared with the $^1P^o$-^1D S XIII transition) and 75.650±0.007 nm (when compared with the $^2S_{1/2}$-$^2P_{1/2}$ S XIV transition). If, in addition, the best value of the $^3S_1$-$^3P_2$ transition of S XV is used as a reference line, we obtain 75.640±0.006 nm.

Wavelength measurements of the $^3S_1$-$^3P_{0,2}$ transition in chlorine were reported previously.[7,8] In the original report the Cl XV $n=8-9$ wavelength was reported as 123.485 nm. Using the revised wavelength reported here, 123.476±0.003 nm, changes the $^3S_1$-$^3P_2$ transition wavelength by −0.004 nm. The disagreement in the previously reported calibration wavelength was caused by the neglect of the lower l transitions in calculating the mean wavelength. A new measurement of the $^3S_1$-$^3P_0$ transition in chlorine is presented.

The final results for silicon, sulfur, and chlorine are given in Table II along with the preliminary values obtained at Notre Dame[22] for these ions, as well as measurements from Oxford[23,24] for $Z=14$.

IV. THEORY

A. Introduction

In one-electron systems, relativistic corrections to the nonrelativistic energy (from the Schrödinger equation) are evaluated directly using the Dirac theory. Contributions which arise when using the more rigorous treatment of QED can be evaluated perturbatively. In this way, the two effects arising when one includes relativity and QED theory are clearly separated from the nonrelativistic energy and from each other.

For two-electron ions, although the nonrelativistic energy is well defined, separating the relativistic and QED contributions is more difficult and not truly possible. QED is completely covariant, and its rigorous application to the two-electron system would include all of these contributions. However, the difficulties associated with an exact treatment have prohibited its use for high-order calculations of these interactions. Thus, for low-Z systems only the ground-state corrections to order α^3 have been obtained[25] and have used nonrelativistic wave functions for their evaluation.[26] Calculations of the α^3 QED corrections have been applied to the $1s2p\ ^3P$ fine-structure intervals in helium.[27] Extrapolations of these α^3 corrections to high Z for all the $n=2$

TABLE II. Results for the $1s2s\ ^3S_1$-$1s2p\ ^3P_{2,0}$ transitions in Si, S, and Cl.

	$^3S_1$-$^3P_2$		$^3S_1$-$^3P_0$	
Z	Wavelength (nm)	Wave number (cm^{-1})	Wavelength (nm)	Wave number (cm^{-1})
14	81.469(2)[a]	122 746 (3)	87.862(3)[a]	113 815 (4)
	81.470(10)[b]	122 745(15)	87.880(20)[b]	113 790(25)
	81.460(10)[c]	122 730(15)	87.860(10)[c]	113 817(13)
	81.450(40)[d]		87.830(60)[d]	
16	67.343(2)[a]	148 493 (5)	75.644(6)[a]	132 198(10)
	67.350(10)[b]	148 480(20)	75.640(20)[b]	132 200(40)
17	61.379(2)[e]	162 923 (6)	70.600(20)[a]	141 643(40)
	61.380(10)[b]	162 920(25)		

[a]This work.
[b]Notre Dame results, Ref. 22.
[c]Armour *et al.*, Ref. 23.
[d]O'Brien *et al.*, Ref. 24.
[e]Berry *et al.*, Refs. 7 and 8.

levels are discussed below.

Much of the theoretical interest in the atomic many-body problem has focused on developing Hamiltonians and operators which can accurately approximate the contributions of relativistic and QED interactions.

Thus, the well-known Breit operator

$$B=(-e^2/2r_{12})[\vec{\alpha}_1\cdot\vec{\alpha}_2+(\vec{\alpha}_1\cdot\vec{r}_{12})(\vec{\alpha}_2\cdot\vec{r}_{12})/r_{12}^2] \tag{11}$$

represents some of the terms corresponding to exchange of transverse photons between the electrons. It has been treated extensively in the literature[28] and has been modified[29,30] to allow calculations to all orders in the external potential. Sucher[30] gives a treatment of the theoretical basis for the Hamiltonians we shall use.

B. Methods of calculation

Formally, we use the Hamiltonian

$$H=\sum H_D(i)+\frac{e^2}{r_{12}}+B+H_{\rm MP}\ , \tag{12}$$

where

$$H_D(i)=(\vec{\alpha}_i\cdot\vec{p}_i+\beta_i mc^2-Ze^2/r_i) \tag{13}$$

is the Dirac single-particle Hamiltonian for each electron ($i=1,2$). The next two terms consist of the nonrelativistic and relativistic electron-electron interactions, respectively. $H_{\rm MP}$ is a mass-polarization term, arising because the center-of-mass motion cannot be completely decoupled:

$$H_{\rm MP}=-\frac{m}{M}(\vec{p}_1\cdot\vec{p}_2) \tag{14}$$

and can be evaluated perturbatively.[28]

We shall use scaled atomic units (s.a.u.), $\hbar=m=Ze^2=1$, such that the velocity of light $c=1/\alpha Z$, where $\alpha=e^2/\hbar c$ and $\alpha^{-1}=137.036\,04(11)$.

The Hamiltonian H can be considered in two parts in two different ways for the high-Z and low-Z ranges of ions: for high Z, we write

$$H=H_{0,\rm rel}+W_{\rm rel}\ , \tag{15}$$

where

$$H_{0,\rm rel}=\sum\left[\frac{\beta_i}{\alpha^2Z^2}+\frac{\vec{\alpha}_i\cdot\vec{p}_i}{\alpha Z}-\frac{1}{r_i}\right] \tag{16}$$

and

$$W_{\rm rel}=Z^{-1}(1/r_{12}\{1-\tfrac{1}{2}[\vec{\alpha}_1\cdot\vec{\alpha}_2+(\vec{\alpha}_1\cdot\vec{r}_{12})(\vec{\alpha}_2\cdot\vec{r}_{12})/r_{12}^2]\})\ . \tag{17}$$

Note that $H_{0,\rm rel}$ is the sum of one-electron Dirac Hamiltonians and $W_{\rm rel}$ is the sum of the Breit and $1/r_{12}$ interactions written in s.a.u.

Alternatively, for low-Z systems we can reduce the Hamiltonian to the Breit-Pauli (BP) approximation, and our Hamiltonian becomes

$$H=H_{0,\rm BP}+W_{\rm BP}\ , \tag{18}$$

where

$$H_{0,\rm BP}=\sum\left[\frac{p_i^2}{2}-\frac{1}{r_i}\right]+Z^{-1}\frac{1}{r_{12}} \tag{19}$$

and

$$W_{\rm BP}=\alpha^2Z^2(H_1+H_2+H_3+H_4+H_5)+H_{\rm MP}\ , \tag{20}$$

with $H_1,\ldots,H_5$ as defined in Ref. 28. In our units, all of the basic operators (β,r,p,s, etc.) are of order unity, except the $\vec{\alpha}$ matrices, which are of order αZ. The choice of the zero-order Hamiltonian should thus depend on the values of the larger perturbation parameter; Z^{-1} for the first or α^2Z^2 for the second. For $Z=27$ they are roughly equal. Thus, near this value both the correlation and relativistic effects are of similar importance.

The Breit-Pauli Hamiltonian was used extensively by Accad *et al.*[31] for the nuclear charges $Z=2-10$, using variational wave functions with as many as 2300 parameters to obtain highly accurate values for the zero-order energy. Applying their wave functions to the expectation values of the perturbative terms they also give results for the relativistic corrections and the mass polarization. The fine structure of the QED corrections of order α^3 is included in their fine-structure intervals. These are given by operators similar to, but not identical with, the Breit operators H_3 and H_5 with an extra multiplicative factor of α/π, and take account just of the electron's anomalous magnetic moment. This work has been extended to all Z ions using the variational perturbation technique to solve the nonrelativistic Hamiltonian as a $1/Z$ ex-

pansion

$$H_{0,\mathrm{BP}}=H_0+Z^{-1}(1/r_{12})\,. \tag{21}$$

Blanchard[32] refined the energy expansions of Sanders and Scherr[33] and of Aashamar[34] to obtain nonrelativistic energies accurate to better than 1 cm^{-1} for intermediate values of Z.

Similarly, we have obtained the mass polarization, relativistic correction, and fine-structure intervals ν_{01} and ν_{21} from an extrapolation of the values of Accad *et al.*[31] using a Padé approximation technique.[32] With the relativistic energies in units of R_m, the reduced mass Rydberg, their data were fit to a rational polynomial of the form

$$E_J=Z^4\left\{a_0+a_1Z^{-1}+Z^{-2}\left[\sum_{i=1}^{N_1}b_iZ^{-i}\Big/\left[1+\sum_{i=1}^{N_2}c_iZ^{-i}\right]\right]\right\}, \tag{22}$$

where the E_J are the energies for $Z=2-10$. The value for a_0 is known exactly, while a_1 can be obtained from the work of Doyle.[35]

For the fine-structure intervals ν_{01} and ν_{21}, the same fitting function is applicable. In order to be consistent, the QED part of these intervals of order α^3, though actually fit in the fitting procedure, was subsequently subtracted off in the final results according to a formula given by Ermolaev[36] which is expected to be accurate for high Z. The total contribution of this α^3 term for $Z=17$ is only 37.5 cm^{-1} for ν_{01} and 10.4 cm^{-1} for ν_{21}.

The larger α^2 contribution to a_0 can be obtained from the difference of the Dirac fine structure for the $(1s_{1/2},2p_{1/2})\,^3P_0$ and $(1s_{1/2},2p_{3/2})\,^3P_2$ states and the diagonal matrix element after transforming to the LS basis, choosing the triplet rather than the singlet value. (This matrix element is the value for a_0 used in the extrapolation of the $^3P_1$ relativistic correction, E_J.) Note that this results in a mixing of the $^1P_1$ and $^3P_1$ levels and is largely responsible for the decay of the latter to the ground state. The coefficients a_i can be similarly obtained from the α^2Z^3 coefficients of Doyle,[35] which are also given in jj coupling.

Of course, no more than nine parameters were fit at one time, though checks were made with less than this maximum. For all extrapolations the final results were insensitive to the values of N_1 and N_2 in Eq. (22) to within a few parts in 10^5. At this level, the results were also in agreement with those of Ermolaev and Jones.[37]

For ions of very high Z, we must take relativistic effects into account as accurately as possible, while the smaller effect of correlation energy may be evaluated perturbatively, along with the Breit interaction.

The Hamiltonian of Eq. (16) gives zero-order wave functions which are antisymmetrized Slater-type product wave functions, whose components are the well known Dirac four-component spinors. Trivially, one also obtains for the zero-order energy, the sum of the Dirac energies of each electron,

$$E_i=\left[1+\frac{\alpha^2Z^2}{[n_i-k_i+(k_i^2-\alpha^2Z^2)^{1/2}]^2}\right]^{-1/2}. \tag{23}$$

Because of the uncorrelated nature of the zero-order wave functions in this approximation the mass-polarization expectation value is zero for the s states. An exposition for a closed-form expression for the evaluation of the first-order perturbation energy was given by Drake.[6]

Using this technique, we have evaluated the diagonal matrix elements of W_{rel} for the $1s_{1/2}ns_{1/2}$, $1s_{1/2}np_{1/2}$, and $1s_{1/2}np_{3/2}$ states ($n=2,3$) for $Z=1-50$. This is the first application of this technique to the $\Delta n=0$ $n\,^3S_1$-$n\,^3P_{0,2}$.

It is well known that both the Dirac energy and wave function can be expressed as power series in α^2Z^2, with the leading terms in the large and small components of the wave function differing by a factor of αZ. Thus, terms in the perturbation interaction which do not mix large and small components result in an expansion in powers of α^2Z^2. The terms in the Breit interaction containing the Dirac matrices $\vec{\alpha}_i$ which do mix large and small components (and so would lead to half-integral powers of $u=\alpha^2Z^2$) enter only quadratically. Hence, the Breit interaction and the zero-order energy can be expanded in integral powers of u.

It is interesting to examine the results of this perturbative technique in the light of this argument. We have fit the obtained perturbation energies for $z=1-50$ to a power series in α^2Z^2. The leading terms are of order Z Ry and α^2Z^3 Ry and can be compared with the similar coefficients obtained with the variational perturbation method. We find the results for the leading coefficient agree with the results of Blanchard[32] to all eight significant figures given there. The results for the second coefficient also agree with the less precise results of Doyle[35] obtained from similar considerations. We

have thus adopted these values in the extrapolation of the relativistic corrections and fine-structure intervals of Accad *et al.*[31]

We have thus shown that with the Breit-Pauli Hamiltonian, one obtains an expansion of the energy which can be written

$$E=\sum_{i=0}^{\infty}\sum_{j=0}^{1}\epsilon_{ij}Z^{-i}(\alpha^2Z^2)^j\,, \tag{24}$$

in Z^2 Ry (reduced mass). While the relativistic Hamiltonian gives the energy in a form

$$E=\sum_{i=0}^{1}\sum_{j=0}^{\infty}\epsilon_{ij}Z^{-i}(\alpha^2Z^2)^j\,, \tag{25}$$

in Z^2 Ry (reduced mass).

It should be noted that there are four common terms in these two expansions ($\epsilon_{00},\epsilon_{01},\epsilon_{10},\epsilon_{11}$). Ermolaev and Jones[38] show that the two techniques are exactly equivalent in these common coefficients, though, of course, only if the nonrelativistic wave functions are exact.

It can be expected that by summing both expansions, taking care to count common terms only once, one can obtain results more accurate than either gives if taken alone.

The final results of this calculation are illustrated in Tables III, IV, and V which show the energies for the $1s\,2s\ ^3S_1$, $1s\,2p\ ^3P_2$, and $1s\,2p\ ^3P_0$ in a manner that illustrates this type of expansion. Terms along the top row are the energies associated with the Dirac equation of zeroth, first, and higher order in α^2Z^2, along with their total. Similarly, the terms in the first column represent the nonrelativistic energy of zeroth, first, and higher order in Z^{-1}, along with their total. Terms in the second row were obtained from the Drake technique and represent the one-photon-exchange term in the Breit interaction to all orders in α^2Z^2. The second column gives all relativistic and Breit corrections of order α^2 obtained from the extrapolation of the relativistic and fine-structure intervals of Accad *et al.*[31] The mass-polarization contribution and the total energy are given separately at the end of each matrix. Extrapolating to the next

TABLE III. $^3S_1$ energy matrix (in cm^{-1}).

	$(\alpha^2Z^2)^0$	$(\alpha^2Z^2)^1$	$(\alpha^2Z^2)^2+\cdots$	Total
		$Z=14$		
Z^2	−26 885 114.13	−73 659.26	−391.55	−26 959 164.95
Z^1	577 426.71	2467.26	14.57	579 908.54
$Z^0+\cdots$	−10 485.36	−96.31		
Total	−26 318 172.8	−71 288.31		
Mass polarization = 0.58				
Total energy = −26 389 837.50				
		$Z=16$		
Z^2	−35 115 337.19	−125 659.76	−874.22	−35 241 871.17
Z^1	659 917.86	3682.92	28.46	663 629.24
$Z^0+\cdots$	−10 474.87	−126.05		
Total	−34 465 894.21	−122 102.89		
Mass polarization = 0.59				
Total energy = −34 588 842.26				
		$Z=17$		
Z^2	−39 641 981.95	−160 144.72	−1259.16	−39 803 385.82
Z^1	701 163.76	4417.53	38.58	705 619.87
$Z^0+\cdots$	−10 470.60	−142.41		
Total	−38 951 288.79	−155 869.60		
Mass polarization = 0.58				
Total energy = −39 108 378.38				

TABLE IV. $^3P_2$ energy matrix (in cm^{-1}).

	$(\alpha^2Z^2)^0$	$(\alpha^2Z^2)^1$	$(\alpha^2Z^2)^2+\cdots$	Total
		$Z=14$		
Z^2	−26 885 114.13	−59 628.93	+299.39	−26 945 042.45
Z^1	693 567.69	1303.26	−0.62	694 870.33
$Z^0+\cdots$	−16 293.15	−107.58		
Total	−26 207 839.59	−58 433.25		
Mass polarization = −56.92				
Total energy = −26 266 629.77				
		$Z=16$		
Z^2	−35 115 337.19	−101 724.57	−668.43	−35 217 730.19
Z^1	792 650.73	1945.39	−1.19	794 594.93
$Z^0+\cdots$	−16 257.82	−140.52		
Total	−34 338 944.29	−99 919.69		
Mass polarization = −66.27				
Total energy = −34 439 599.87				
		$Z=17$		
Z^2	−39 641 981.95	−129 640.96	−962.73	−39 772 585.64
Z^1	842 192.64	2333.43	−1.61	844 524.46
$Z^0+\cdots$	−16 243.40	−158.64		
Total	−38 816 032.71	127 466.17		
Mass polarization = −68.92				
Total energy = −38 944 532.14				

higher rows and columns indicates a probable error in the total energy of less than 5 cm^{-1} for the $^3S_1$ and $^3P_2$ states, and slightly larger for the $^3P_0$ state. Uncertainties in the extrapolation of the relativistic corrections are probably also less than 5 cm^{-1}.

C. Lamb shift

We have previously discussed[7,8] the one-electron part of the Lamb-shift corrections. The results for the $1s\,2s\ ^3S_1$-$1s\,2p\ ^3P_{0,2}$ transition for $Z=2-50$ are shown in Table VI, together with the results of the calculations of Sec. III B. The total energy updates that which is given in Ref. 8 which contains errors due to double counting of some QED fine-structure corrections and some typographical mistakes.

In Table VII, we show the difference between experiment and the theoretical values of Table VI for the energies of the transitions $1s\,2s\ ^3S_1$-$1s\,2p\ ^3P_{0,2}$. These differences ΔP_0 and ΔP_2 indicate an approximate Z^3 dependence; this can also be seen from the quantities $Q_i=(\Delta P_i/Z^3)100$, $(i=0,2)$ which are shown in Table VII and in Figs. 9 and 10. We note that the difference between experiment and theory is 45 cm^{-1} for S XV, far outside the estimated experimental error of ± 5 cm^{-1}. This Z^3 discrepancy was first noted by J. Silver for ions of $Z \leq 10$ (private communication).[39]

We have considered possible omissions from the theory which could give rise to such discrepancies: two-photon-exchange or second-order Breit terms which would contribute energy corrections to the double series expansion are estimated[40] to be of the order of 5 cm^{-1} and insufficient alone to account for the discrepancies. The first-order corrections to the Lamb shift correspond approximately to the lowest-order shielding corrections of the Lamb shift. As for the non-QED terms they also contribute at the $1/Z$ level. We briefly sketch an estimate of the α^3Z^3 and α^4Z^4 corrections for the α^3Z^4 and α^4Z^5 one-electron self-energy and vacuum-polarization terms.

Using the nonrelativistic density of the electron at the nucleus $\delta^3_{nl}(r)=\delta_{l0}Z^3/\pi n^3$ to illustrate the contact terms of the Lamb shift, we may write the two lowest-order, one-electron terms[41] in the form

TABLE V. $^3P_0$ energy matrix (in cm^{-1}).

	$(\alpha^2Z^2)^0$	$(\alpha^2Z^2)^1$	$(\alpha^2Z^2)^2+\ldots$	Total
		$Z=14$		
Z^2	−26 885 114.13	−73 659.26	−391.55	−26 959 164.95
Z^1	693 567.69	7047.82	48.21	700 663.72
$Z^0+\cdots$	−16 293.15	−682.25		
Total	−26 207 839.59	−67 293.70		
Mass polarization = −56.92				
Total energy = −26 275 533.55				
		$Z=16$		
Z^2	−35 115 337.19	−125 659.76	−874.22	−35 241 871.17
Z^1	792 650.73	10 520.38	94.22	803 265.33
$Z^0+\cdots$	−16 257.82	−894.03		
Total	−34 338 944.29	−116 033.40		
Mass polarization = −66.27				
Total energy = −34 455 823.96				
		$Z=17$		
Z^2	−39 641 981.95	−160 144.72	−1259.16	−39 803 385.82
Z^1	842 192.64	12 618.83	127.75	854 939.21
$Z^0+\cdots$	−16 243.40	−1 010.70		
Total	−38 816 032.71	−148 536.59		
Mass polarization = −68.92				
Total energy = −38 965 769.62				

$$E(n,l)=(8\alpha^3Z/3)\delta^3_{nl}(r)[\tfrac{19}{30}-2\ln(\alpha Z)+3\pi\alpha Z(\tfrac{427}{384}-0.5\ln 2)]$$
$$+(8\alpha^3Z^4/3\pi n^3)\{\ln[Z^2/K_0(n,l)]+(1-\delta_{10})3C_{lj}/[8(2l+1)]\}\ \mathrm{Ry}\ , \tag{26}$$

where

$$C_{lj}=\begin{cases}(l+1)^{-1} & \text{for } j=l+\frac{1}{2}\ ,\\ -l^{-1} & \text{for } k=l-\frac{1}{2}\ .\end{cases} \tag{27}$$

The extension to the two-electron Lamb shift is then taken as[41,36]

$$E(1s,nl)=(8\alpha^3Z/3)\langle\delta^3(r_1)+\delta^3(r_2)\rangle\{\tfrac{19}{30}-2\ln(\alpha Z)+\ln[Z^2/K_0(1s,nl)]+3\pi\alpha Z(\tfrac{427}{384}-0.5\ln 2)\}$$
$$+(8\alpha^3Z^4/3\pi n^3)(1-\delta_{\mathrm{LO}})(1-\delta_{\mathrm{SO}})3[A_{L,J}+(B_{L,J}-3A_{L,J})Z^{-1}]/[8L(L+1)(2L+1)]\ , \tag{28}$$

where

$$A_{L,L+1}=L,\quad B_{L,L+1}=-4L(L+1)/(2L+3),$$
$$A_{L,L}=-1,\quad B_{L,L}=0, \tag{29}$$
$$A_{L,L-1}=-(L+1),\quad B_{L,L-1}=4L(L+1)/(2L-1)\ .$$

Excluded terms include electron-electron contact terms (which vanish for the triplet states) and higher-order corrections in Z^{-1}, for the fine structure, along with all corrections of higher order in α and αZ.

Thus in order to obtain the Lamb shift for a

TABLE VI. $1s\,2s\ ^3S_1$-$1s\,2p\ ^3P_{0,2}$ transitions—theoretical values, neglecting two-electron QED corrections (in cm^{-1}). The QED values for $^3S_1$-$^3P_2$ also include the J-dependent corrections as evaluated by Garcia and Mack, J. Opt. Soc. Am. 55, 654 (1965).

	$^3S_1$-$^3P_2$			$^3S_1$-$^3P_0$		
Z	Non-QED	One-El. QED	Total	Non-QED	One-El. QED	Total
2	9 223.955	−0.46	9 223.50	9 225.021	−0.47	9 224.55
3	18 229.22	−2.02	18 227.20	18 232.34	−2.09	18 230.25
4	26 872.18	−5.78	26 866.40	26 868.91	−6.00	26 862.91
5	35 440.36	−12.97	35 427.39	35 404.13	−13.49	35 390.64
6	44 042.8	−25.00	44 017.81	43 920.11	−26.08	43 894.03
7	52 757.28	−43.40	52 713.87	52 458.86	−45.41	52 413.45
8	61 650.21	−69.84	61 580.36	61 042.22	−73.26	60 968.96
9	70 794.3	−106.09	70 688.21	69 689.39	−111.51	69 577.87
10	80 260.59	−153.91	80 106.68	78 408.93	−162.15	78 246.78
11	90 141.16	−215.12	89 926.04	87 221.43	−227.12	86 994.31
12	100 520.8	−291.83	100 228.9	96 131.08	−308.74	95 822.34
13	111 508.9	−385.95	111 122.9	105 157.5	−409.11	104 748.4
14	123 207.7	−499.60	122 708.1	114 303.9	−530.58	113 773.3
15	135 745.3	−634.99	135 110.3	123 589.9	−675.59	122 914.3
16	149 242.4	−794.10	148 448.3	133 018.3	−846.35	132 171.9
17	163 846.2	−979.43	162 866.8	142 608.8	−1045.62	141 563.2
18	179 704.9	−1193.20	178 511.7	152 372	−1275.88	151 096.1
19	196 961.7	−1436.81	195 524.9	162 304.3	−1538.80	160 765.5
20	215 800.5	−1714.05	214 086.4	172 432.2	−1838.45	170 593.7
21	236 405.1	−2026.59	234 378.5	182 772.1	−2176.79	180 595.3
22	258 952.6	−2377.06	256 575.4	193 323	−2556.76	190 766.2
23	283 647.2	−2767.00	280 880.2	204 100.9	−2980.17	201 120.7
24	310 696.3	−3200.79	307 495.5	215 113.9	−3451.74	211 662.2
25	340 328.1	−3680.14	336 648.0	226 379.8	−3973.48	222 406.3
26	372 749.2	−4206.38	368 542.8	237 883.9	−4547.06	233 346.8
27	408 323	−4785.14	403 537.9	249 756.4	−5178.43	244 578.0
28	447 132.2	−5414.22	441 718.0	261 835.6	−5865.71	255 969.9
29	489 553.7	−6106.86	483 446.8	274 241.2	−6622.50	267 618.7
30	535 840.3	−6853.20	528 987.1	286 957.4	−7439.25	279 518.1
31	586 302.2	−7667.6	578 634.6	300 012.3	−8330.73	291 681.6
32	641 239.5	−8545.2	632 694.3	313 411.5	−9292.29	304 119.2
33	700 967.4	−9491.4	691 474.0	327 162.6	−10 329.8	316 832.8
34	765 836.2	−10 512.2	755 324.0	341 294	−11 449.6	329 844.4
35	836 178.9	−11 606.1	824 572.8	355 803.4	−12 650.5	343 152.9
36	912 382.1	−12 784.9	899 597.2	370 727	−13 944.3	356 782.7
37	994 808.4	−14 038.8	980 769.6	386 063	−15 322.8	370 740.2
38	1083 865	−15 386	1068 479	401 837.9	−16 803.2	385 034.7
39	1179 957	−16 815	1163 142	418 061.2	−18 375.6	399 685.6
40	1283 516	−18 346	1265 170	434 753.3	−20 059.5	414 693.8
41	1394 995	−19 976	1375 019	451 935.3	−21 851.6	430 083.7
42	1514 855	−21 229	1493 626	469 625	−23 772.3	445 852.7
43	1643 571	−23 563	1620 008	487 831.8	−25 796.9	462 034.9
44	1781 650	−25 530	1756 120	506 579.9	−27 958.7	478 621.2
45	1929 612	−27 597	1902 015	525 886.9	−30 234.7	495 652.2
46	2088 003	−29 819	2058 184	545 778.1	−32 678.9	513 099.2
47	2257 380	−32 131	2225 249	566 266.8	−35 221.6	531 045.2
48	2438 342	−34 629	2403 713	587 388.9	−37 990.1	549 398.8
49	2631 474	−37 233	2594 241	609 143.8	−40 853.3	568 290.5
50	2837 422	−40 006	2797 416	631 568.1	−43 935.7	587 632.4

multielectron atom, we need to evaluate the electron density at the nucleus and the Bethe logarithm term $K_0(n,l)$. From the $1/Z$ variational expansion we can use the nonrelativistic values for the two-electron system,[30]

$$\pi\langle\delta^3(r_1)+\delta^3(r_2)\rangle=\sum_i \frac{Z^3}{n_i^3}\delta_{l_i,0}+aZ^2+bZ+\cdots . \tag{30}$$

The second term in this expansion yields part of the first-order screening correction to the one-electron Lamb shift. The largest term is proportional to Z^3.

Evaluation of $K_0(n,l)$ requires calculation of the sum

$$S_i=\sum_n f_{in}\nu_{in}^2\ln|\nu_{in}| , \tag{31}$$

where f_{in} is the oscillator strength from the level of interest i to leven n, and ν_{in} is the energy difference; the sum is taken over all discrete states and continua. Calculation of S_i is, in general, difficult for systems of more than one electron, and has only been attempted[42] for a few states in helium and Li^+.

We choose K_0 to be of the Z-expansion form suggested by Bethe and Salpeter,[28] but with its leading term adjusted to give a Z^4 dependence of the Lamb-shift equation (26) in agreement with the one-electron Lamb shift. For example, for the

TABLE VII. Differences between theory (neglecting two-electron QED corrections) and experiment (in cm^{-1}) for the $1s\,2s\ ^3S_1$-$1s\,2p\ ^3P_{0,2}$ transitions.

	$(E_{expt}-E_{theor})$ cm^{-1}		$Q_2=\left[\frac{\Delta P_2}{Z^3}\right]100$	$Q_0=\left[\frac{\Delta P_0}{Z^3}\right]100$
	$2s\ ^3S_1$-$2p\ ^3P_2$	$2s\ ^3S_1$-$2p\ ^3P_0$		
Ion	ΔP_2	ΔP_0		
Be III	1.5(0.2)[a]	4.5(0.7)[a]	2.34(0.3)	7.03(1.1)
B IV	2.1[b]	2.6[b]	1.68	2.08
C V	3.8(1.0)[c]	5.0(1.0)[c]	1.76(0.5)	2.31(0.5)
N VI	5.6(0.6)[d]	0.4(1.4)[d]	1.63(0.2)	0.12(0.4)
O VII	14.9(0.8)[d]	10.3(3.0)[d]	2.93(0.2)	2.01(0.6)
F VIII	12.2(3.0)[e]	8.1(4.0)[e]	1.65(0.4)	1.10(0.4)
Ne IX	13.8(1.3)[e]	20.1(2.5)[e]	1.38(0.13)	2.01(0.25)
Al XII	−13 (100)[f]	182 (100)[f]	−0.6(4.6)	8.28(4.6)
Si XIII	37 (15)[g]	17 (25)[g]	1.35(0.6)	0.62(0.9)
	27 (15)[h]	29 (15)[h]	0.98(0.6)	1.06(0.6)
	38 (4)	42 (5)[i]	1.38(0.2)	1.53(0.2)
S XV	45 (5)[i]	27 (12)[i]	1.10(0.12)	0.66(0.3)
Cl XVI	57 (6)[j]	80 (40)[i]	1.16(0.12)	1.63(0.8)
Ar XVII	−10 (300)[k]	256 (250)[k]	−0.2(5.1)	4.4(4.4)
Fe XXV	433 (125)[l]	−763 (550)[l]	2.46(0.71)	−4.34(3.1)

[a]B. Löfstrand, Phys. Scr. 8, 57 (1973).
[b]Edlén, Nova Acta Regiae Soc. Sci. Ups. 9, (1934).
[c]B. Edlén and B. Lofstränd, J. Phys. B 3, 1380 (1970).
[d]S. C. Baker, J. Phys. B 6, 709 (1973).
[e]W. Engelhardt and J. Sommer, Astrophys. J. 167, 201 (1971).
[f]B. Denne, S. Huldt, J. Pihl, and R. Hallin, Phys. Scr. 22, 45 (1980).
[g]Reference 22.
[h]Reference 23.
[i]This work.
[j]Reference 8 and this work.
[k]W. A. Davis and R. Marrus, Phys. Rev. A 15, 1963 (1977).
[l]J. P. Buchet *et al.*, Ref. 44, p. 236, and J. P. Buchet, M. C. Buchet-Poulizac, A. Denis, J. Désesquelles, M. Druetta, J. P. Grandin, and X. Husson, Phys. Rev. A 23, 3354 (1981).

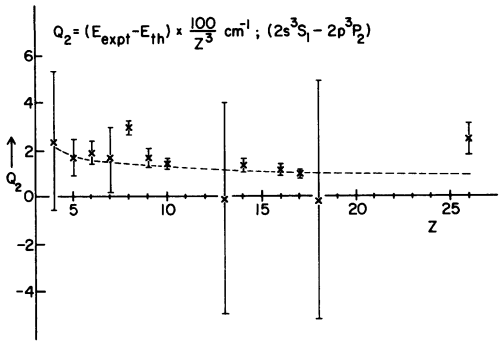

FIG. 9. Experiment—theory for $1s\,2s\ ^3S_1$-$1s\,2p\ ^3P_2$ (scaled by Z^3) versus Z.

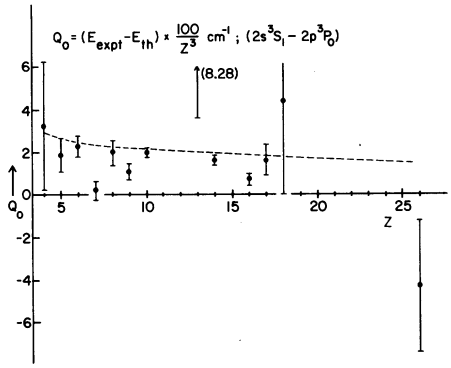

FIG. 10. Experiment—theory for $1s\,2s\ ^3S_1$-$1s\,2p\ ^3P_0$ (scaled by Z^3) versus Z.

$1s\,2p$ state we write

$$\lim_{Z\to\infty} \ln K_0(1s\,2p) = \ln K_0(1s) + \frac{1}{2^3}\ln K_0(2p) \qquad (32)$$

leading to

$$K_0(1s\,2p) = 19.186Z^2(1 + d/Z^2 \cdots)^2 . \qquad (33)$$

The results of the calculations for $1s\,2s\ ^3S_1$-$1s\,2p\ ^3P_{0,2}$ are listed in Table VIII and are shown

TABLE VIII. Two-electron Lamb-shift contribution to the $1s\,2s\ ^3S_1$-$1s\,2p\ ^3P_{0,2}$ (in cm^{-1}).

	$^3S_1$-$^3P_2$		$^3S_1$-$^3P_0$	
Z	Theory	Expt.[a]	Theory	Expt.[a]
2	0.21		0.26	
3	0.63		0.77	
4	1.34	1.5(0.2)	1.68	4.5(0.7)
5	2.40	2.1	3.05	2.6
6	3.84	3.8(1.0)	4.97	5.0(1.0)
7	5.70	5.6(0.6)	7.50	0.4(1.4)
8	8.01	14.9(0.8)	10.70	10.3(3.0)
9	10.80	12.2(3.0)	14.64	8.1(4.0)
10	14.11	13.8(1.3)	19.37	20.1(2.5)
11	17.95		24.95	
12	22.36		31.45	
13	27.37	−13(100)	38.92	182(100)
14	33.00	38(4)	47.44	42(5)
15	39.29		57.05	
16	46.28	45(5)	67.82	27(12)
17	53.99	57(6)	79.84	80(40)
18	62.5	−10(300)	93.2	256(250)
19	71.8		107.8	
20	81.9		124.0	
21	92.9		141.7	
22	104.9		160.9	
23	117.9		181.9	
24	131.9		204.7	
25	147.1		229.3	
26	163.4	433(125)	255.9	−763(550)

[a]Experimental data as given in Table VII.

as the dashed curves in Figs. 9 and 10. Note that Eq. (28) consists of two principal terms each of which is expanded in powers of $1/Z$. Each leading term is the hydrogenic term, proportional to Z^4/n^3, which has been subtracted to give the two-electron corrections of Table VIII. The last term of Eq. (28) has been adjusted to be consistent with the work of Ermolaev[36,41] to order Z^3. The uncertain contribution from the correction to the Bethe log term [d in Eq. (8)] is neglected. Crude estimates (from calculations at $Z=2$) of its effect indicate a probable upward shift of this curve of approximately 10–20%. However, it should be noted that higher-order ($Z\alpha$) corrections to the one-electron Lamb shift at $Z=17$ constitute more than 10% of the total and hence the two-electron, $1/Z$ correction to these terms should also become important, especially for the higher-Z ions.

V. SUMMARY AND CONCLUSION

This work concludes this stage of our precision wavelength measurements of the $1s\,2s\ ^3S_1$-$1s\,2p\ ^3P_{0,2}$ transitions in the heliumlike ions of silicon, sulfur, and chlorine. We have attained accuracies of 4–6 cm^{-1} for the $^3P_2$ transitions and 5–30 cm^{-1} for the $^3P_0$ transitions. Improved precision may be possible only with improved knowledge of relative populations and fine structures of the high Rydberg transitions, or of experimental precision of resonance-line wavelengths of lower-charge-state ions. Problems from the dispersion of the monochromator and signal-to-noise ratios may be reduced by multiplexing the signals with a position sensitive detector in the exit focal plane of the monochromator. This reduces the grating screw problem, and enhances the signal-to-noise ratio for a given ion-beam flux. We have made initial measurements of this type.[43]

We have shown that accurate tests of QED in strong electromagnetic fields can be obtained from fine-structure measurements in medium-Z ions. Current theoretical limitations lie in calculations of the two-electron Lamb-shift terms.

We have demonstrated the usefulness of a double series expansion of the "known" (Coulomb and Breit) interactions, in powers of the correlation and relativistic parameters, Z^{-1} and α^2Z^2, respectively. Through extrapolation of the Breit interaction of order α^2 from lower values of Z, and actual calculation of the one-photon-exchange part of the Breit interaction to all orders in α^2Z^2, we have reduced the uncertainty in these non-Lamb-shift terms to the level of the experimental precision.[44]

Using a similar approach to the calculation of the Lamb-shift contributions, we use the one-electron Lamb-shift calculation and attempt to obtain correlation corrections to it. This arises naturally from the correlation correction to the density of the electrons at $r=0$, used in the one-electron contact interactions of the Lamb shift and leads to a technique to extrapolate the Bethe logarithm so that the leading term of the two-electron Lamb shift is in agreement with the one-electron values. We find that we can reduce the discrepancies between theory and experiment to approximately the level of the experimental precision by including α^3Z^3 and α^4Z^4 corrections to the corresponding α^3Z^4 and α^4Z^5 one-electron Lamb-shift values (which contribute $\simeq$90% to the total).

There are relatively few measurements of QED in the strong-field limit where perturbative approaches based on a weak-coupling coefficient may eventually break down. With new or improved experimental techniques and two-electron Lamb-shift calculations, these measurements and measurements in other high-Z ions of few electrons can be expected to provide the most demanding requirements of this fundamental theory of physics in atomic systems.[45]

ACKNOWLEDGMENTS

We wish to thank Ed Berners (at Notre Dame) and Jim Ray (at Argonne) for their technical assistance in the experiments. Kwok Tsang Cheng, Walter Johnson, and Gordon Drake were very helpful in elucidating many of the theoretical aspects. This work was supported by the U. S. Department of Energy, Office of Basic Energy Sciences, under Contract No.W-31-109-Eng-38.

---

*This work was submitted in partial fulfillment of the requirements for the Doctor of Philosophy degree, Department of Physics, Division of the Physical Sciences, University of Chicago. Present address: Department of Physics, University of Arizona, Tucson, Arizona 85721.

†Also at Department of Physics, University of Chicago, Chicago, Illinois 60637.

[1]T. Fulton and R. Karplus, Phys. Rev. 93, 1109 (1954).

[2]P. C. Martin and J. Schwinger, Phys. Rev. 95, 811 (1954).

[3]P. Mohr, Phys. Rev. Lett. 34, 1050 (1975).
[4]G. W. Erickson, J. Phys. Chem. Ref. Data 831 (1977).
[5]See, e.g., H. A. Bethe and E. E. Salpeter, *Quantum Mechanics of One- and Two-Electron Systems* (Plenum, New York, 1977).
[6]See, e.g., G. W. F. Drake, Phys. Rev. A 19, 1387 (1979).
[7]H. G. Berry, R. DeSerio, and A. E. Livingston, Phys. Rev. Lett. 41, 1652 (1978).
[8]H. G. Berry, R. DeSerio, and A. E. Livingston, Phys. Rev. A 22, 198 (1980).
[9]R. DeSerio, Appl. Opt. 20, 1781 (1981); A. E. Livingston and S. J. Hinterlong, *ibid.* 20, 1727 (1981).
[10]J. A. Leavitt, J. W. Robson, and J. O. Stoner, Nucl. Instrum. Methods 110, 423 (1973).
[11]M. Dufay, A. Denis, and J. Désesquelles, Nucl. Instrum. Methods 90, 85 (1970).
[12]H. G. Berry and C. H. Batson, in *Beam-Foil Spectroscopy,* edited by I. A. Sellin and D. J. Pegg (Plenum, New York, 1975), Vol. 1, p. 367.
[13]W. N. Lennard and C. L. Cocke, Nucl. Instrum. Methods 110, 137 (1973).
[14]B. Edlén, in *Handbuch der Physik,* edited by S. Flugge (Springer, Berlin, 1964), Vol. 27.
[15]See, e.g., A. Dalgarno, Adv. Phys. 11, 281 (1962).
[16]B. Edlén, Phys. Scr. 19, 255 (1979).
[17]E. E. Veje, Phys. Rev. A 14, 2077 (1976), and references contained therein.
[18]D. J. Pegg, J. P. Forester, S. B. Elston, P. M. Griffin, K. O. Groeneveld, R. S. Peterson, R. S. Thoe, C. R. Vane, and I. A. Sellin, Astrophys. J. 214, 331 (1977).
[19]R. C. Fawcett, J. Phys. B 3, 1152 (1970).
[20]K. G. Widing and J. D. Purcell, Astrophys. J. 204, L151 (1976).
[21]G. D. Sandlin, G. E. Brueckner, V. E. Scherrer, and R. Tousey, Astrophys. J. 205, L47 (1976).
[22]A. E. Livingston, S. J. Hinterlong, J. A. Poirier, R. DeSerio, and H. G. Berry, J. Phys. B 13, L139 (1980).
[23]I. A. Armour, E. G. Myers, J. D. Silver, and E. Träbert, Phys. Lett. 75A, 45 (1979).
[24]R. O'Brien, J. D. Silver, N. A. Jelley, S. Bashkin, E. Träbert, and P. H. Heckmann, J. Phys. B 12, L41 (1979).
[25]P. K. Kabir and E. E. Salpeter, Phys. Rev. 108, 1256 (1957).
[26]H. Araki, Prog. Theor. Phys. 17, 619 (1957).
[27]G. Araki, M. Ohta, and K. Mano, Phys. Rev. 116, 651 (1959); see also L. Hambro, Phys. Rev. A 5, 2027 (1972), and M. L. Lewis and P. H. Serafino, *ibid.* 18, 867 (1978).
[28]H. A. Bethe and E. E. Salpeter, *Quantum Mechanics of One- and Two-Electron Systems* (Plenum, New York, 1977); pp. 170ff.
[29]M. H. Mittleman, Phys. Rev. A 4, 897 (1971); 5, 2395 (1972).
[30]J. Sucher, Phys. Rev. A 22, 348 (1980).
[31]Y. Accad, C. L. Pekeris, and B. Schiff, Phys. Rev. A 4, 516 (1971); 11, 1479 (1975).
[32]P. Blanchard, Phys. Rev. A 13, 1698 (1976).
[33]F. C. Sanders and C. W. Scherr, Phys. Rev. 181, 84 (1969).
[34]K. Aashamar, J. Midtdal, and G. Lyslo, J. Chem. Phys. 61, 1345 (1974); 52, 3324 (1970).
[35]H. T. Doyle, Adv. At. Mol. Phys. 5, 337 (1969).
[36]A. M. Ermolaev, Phys. Rev. A 8, 1651 (1973).
[37]A. M. Ermolaev and M. Jones, J. Phys. B 7, 199 (1974).
[38]A. M. Ermolaev and M. Jones, J. Phys. B 6, 1 (1973).
[39]See also M. F. Stamp, I. A. Armour, N. J. Peacock, and J. D. Silver, J. Phys. B (in press).
[40]Tables IV and V show that for S XV, the highest-order terms calculated are of the order of 20 cm^{-1} and that the missing terms should be approximately an order of magnitude lower.
[41]A. M. Ermolaev, Phys. Rev. Lett. 34, 380 (1975); he uses a different approach for the K term.
[42]See Ref. 40 and H. G. Berry and R. Bacis, Phys. Rev. A 8, 36 (1973) for summaries of earlier work.
[43]A. E. Livingston, IEEE Trans. Nucl. Sci. NS-28, 1559 (1981).
[44]U. I. Safronova, Phys. Scr. 23, 241 (1981), and earlier work quoted therein gives a more approximate but similar calculation for all the $n=2$ states of helium-like ions for $Z=10-42$.
[45]See, for example, the Proceedings of the Workshop on Foundations of the Relativistic Theory of Atomic Structure, Argonne, Illinois, 1980, edited by H. G. Berry, K. T. Cheng, W. R. Johnson, and Y. K. Kim, Report No. ANL-80-126 (unpublished).